

Communication

**Effect of Length and Contact Chemistry on the Electronic Structure and Thermoelectric Properties of Molecular Junctions**

Aaron Christopher Tan, Janakiraman Balachandran, Seid Hossein Sadat, Vikram Gavini, Barry Dov Dunietz, Sung-Yeon Jang, and Pramod Reddy

*J. Am. Chem. Soc.*, **Just Accepted Manuscript** • DOI: 10.1021/ja202178k • Publication Date (Web): 12 May 2011

Downloaded from <http://pubs.acs.org> on May 14, 2011

**Just Accepted**

“Just Accepted” manuscripts have been peer-reviewed and accepted for publication. They are posted online prior to technical editing, formatting for publication and author proofing. The American Chemical Society provides “Just Accepted” as a free service to the research community to expedite the dissemination of scientific material as soon as possible after acceptance. “Just Accepted” manuscripts appear in full in PDF format accompanied by an HTML abstract. “Just Accepted” manuscripts have been fully peer reviewed, but should not be considered the official version of record. They are accessible to all readers and citable by the Digital Object Identifier (DOI®). “Just Accepted” is an optional service offered to authors. Therefore, the “Just Accepted” Web site may not include all articles that will be published in the journal. After a manuscript is technically edited and formatted, it will be removed from the “Just Accepted” Web site and published as an ASAP article. Note that technical editing may introduce minor changes to the manuscript text and/or graphics which could affect content, and all legal disclaimers and ethical guidelines that apply to the journal pertain. ACS cannot be held responsible for errors or consequences arising from the use of information contained in these “Just Accepted” manuscripts.



# Effect of Length and Contact Chemistry on the Electronic Structure and Thermoelectric Properties of Molecular Junctions

Aaron Tan<sup>1</sup>, Janakiraman Balachandran<sup>2</sup>, Seid Sadat<sup>2</sup>, Vikram Gavini<sup>1,2</sup>, Barry D. Dunietz<sup>\*,3</sup>, Sung-Yeon Jang<sup>‡,4</sup>, Pramod Reddy<sup>#,1,2</sup>

<sup>1</sup>Department of Materials Science and Engineering, University of Michigan, Ann Arbor, Michigan 48109, <sup>2</sup>Department of Mechanical Engineering, University of Michigan, Ann Arbor, Michigan 48109, <sup>3</sup>Department of Chemistry, University of Michigan, Ann Arbor, Michigan 48109, and

<sup>4</sup>Department of Chemistry, Kookmin University, Seoul, Korea

\* E-mail: bdunietz@umich.edu, # E-mail: vikramg@umich.edu, ‡ E-mail: syjang@kookmin.ac.kr, † E-mail: pramodr@umich.edu

KEYWORDS (“Thermoelectric”, “Molecular Junction”, “Electronic structure”, “Electrical conductance”, “Seebeck”).

**ABSTRACT.** We present a combined experimental and computational study that probes the thermoelectric and electrical transport properties of molecular junctions. Experiments were performed on junctions created by trapping aromatic molecules between gold (Au) electrodes. The end groups (–SH, –NC) of the aromatic molecules were systematically varied to study the effect of contact coupling strength and contact chemistry. When the coupling of the molecule with one of the electrodes was reduced by switching the terminal chemistry from –SH to –H, the electrical conductance of molecular junctions decreased by an order of magnitude, whereas the thermopower varied by only a few percent. This observation, which provides information about the effect of contact coupling on the electronic structure of the junctions, has been predicted computationally in the past and is experimentally demonstrated for the first time. Further, our experiments and computational modeling indicate the prospect of tuning thermoelectric properties at the molecular scale. In particular, the thiol terminated aromatic molecular junctions revealed a positive thermopower that increased linearly with length. This positive thermopower is associated with charge transport primarily through the highest occupied molecular orbital (HOMO) as shown by our computational results. In contrast, a negative thermopower was observed for a corresponding molecular junction terminated by an isocyanide group due to charge transport primarily through the lowest unoccupied molecular orbital (LUMO).

Novel charge and energy transport phenomena—with important technological applications—are expected to arise in nanometer-sized molecular junctions. Negative differential resistance<sup>1</sup>, rectification<sup>2</sup>, switching<sup>3</sup>, and gating<sup>4</sup> have all been observed in specific molecular junctions and present great potential in advancing electronic applications. In addition to these important molecular-electronic phenomena, recent computational studies<sup>5–8</sup> suggest that it should be possible to create junctions with large thermoelectric efficiencies using appropriately tailored organic molecules.

Understanding the structure-property relationship in molecular junctions is a critical step in achieving these important technological goals. It is well known that the chemical structure of molecular junctions plays an important role in determining their transport properties<sup>9–14</sup>. Recently, the dependence of electrical conductance on the structure of molecular junctions has been extensively probed using a variety of experimental techniques.<sup>9,12,13,15</sup> These experiments provide important

insights into the dependence of electrical conductance on the molecular backbone, end groups, and metal contacts. However, the relationship between thermoelectric properties and the molecular structure and contact chemistry of junctions has remained relatively unexplored.

In this communication, we probe the dependence of junction thermoelectric properties on molecular length and contact coupling chemistry using a combined experimental and computational approach. We analyze the electrical conductance and thermopower of a series of molecular junctions using a novel atomic force microscope (AFM) based technique<sup>16</sup> that enables monolayer measurements not accessible in previous thermopower experiments.<sup>10</sup> In our AFM technique, molecular junctions are created by first self assembling aromatic molecules into a monolayer on a gold substrate and placing them in contact with a gold-coated AFM tip (Figure 1a). Approximately 100 molecules are trapped by using an AFM tip with a radius of ~70 nm and by controlling the contact force to be ~1 nN. Further details are provided in the Supporting Information (SI). Subsequently, known temperature differentials are imposed across the molecular junctions to measure the resulting thermoelectric voltages from which the thermopower<sup>16</sup> (voltage output per unit temperature differential, also known as the Seebeck coefficient) is obtained. Alternately, a voltage differential is applied to obtain the current-voltage (I-V) characteristics<sup>17</sup> and the electrical resistance of junctions. The molecules used in this work (Figure 1b) are either singly or doubly terminated with thiol (–SH) or isocyanide (–NC) end groups. Various junctions created from these molecules were probed to study the thermoelectric structure-property relationship of junctions. In addition to the experiments, we computationally model the molecular junctions to obtain insight into the effect of electronic structure on transport properties. In our modeling, the electrical conductance and thermoelectric properties of molecular junctions are obtained by an approach that combines density functional theory (DFT) with a Green’s function technique<sup>18–21</sup> implementing the Landauer formalism of transport (see SI for details). A representative model of the junctions used in our calculations is provided in Figure 1c.

Thermoelectric measurements provide additional insights into the electronic structure of molecular junctions that cannot be obtained by electrical transport measurements alone. Specifically, conductance measurements cannot uniquely identify<sup>10,22</sup> whether the HOMO orbital or the LUMO orbital lies closer to the Fermi level. However, thermoelectric measurements can answer this question. As will be subsequently discussed in this work, a positive thermopower is associated with a HOMO that is closer to the chemical potential, indicating hole dominated (p-type) transport. In the other scenario, transport is

LUMO dominated (n-type) and is related to a negative thermopower. Figure 1d illustrates the two scenarios that thermoelectric measurements can be used to distinguish.

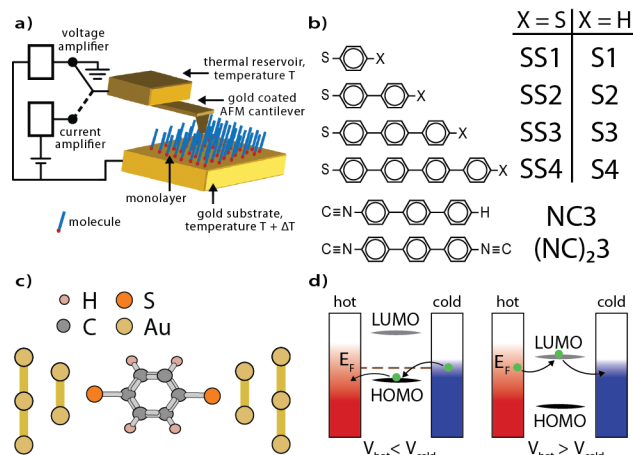


**Figure 1.** a) A schematic of the experimental setup for the measurement of the electrical conductance and Seebeck coefficient. b) The thiol and isocyanide terminated aromatic molecules studied in this work. c) A schematic of the model used for computing the transport properties of the Au-SS1-Au junction. d) The two scenarios that a Seebeck coefficient measurement can distinguish are illustrated: HOMO closer to the Fermi level results in a positive Seebeck coefficient whereas the other scenario results in a negative Seebeck coefficient.

*Effect of molecular length on electrical conductance and thermopower (Seebeck coefficient).* The length dependence of the electrical conductance and Seebeck coefficient of molecular junctions is probed by trapping thiol terminated aromatic molecules (SS1, SS2, SS3, shown in Figure 1b) between gold electrodes. The measured resistances of the junctions increase exponentially with the length of the molecules as shown in Figure 2a. The transport properties of molecular junctions were computationally studied using the Landauer formalism. In this approach, the electrical current ( $I$ ), the electrical conductance ( $G$ ), and the thermopower ( $S$ ) of a molecular junction are expressed as<sup>22</sup>

$$I = \frac{2e}{h} \int_{-\infty}^{\infty} \tau(E) [f_1(E) - f_2(E)] dE \quad (1)$$

$$G = \frac{2e^2}{h} \tau(E_F); \quad S = -\frac{\pi^2 k_B^2 T}{3|e|} \frac{1}{\tau(E)} \left. \frac{\partial \tau(E)}{\partial E} \right|_{E=E_F} \quad (2)$$

where  $\tau(E)$  is the transmission function,  $f_1(E)$  and  $f_2(E)$  are the Fermi-Dirac distributions corresponding to the electrodes,  $k_B$  is the Boltzmann constant,  $e$  is the charge of an electron,  $h$  is the Planck constant,  $T$  is the average absolute temperature of the junction, and  $E_F$  is the energy corresponding to the Fermi level of the electrodes. The computed transmission functions,  $\tau(E)$ , for junctions based on SS1 to SS4 molecules are shown in Figure 2b. The transmission at  $E_F$  decreases rapidly as the length of the molecules is increased, explaining the observed sharp increase in the resistance of the molecular junctions.

The measured thermoelectric voltages ( $\Delta V$ ) for the thiol terminated molecular junctions, as a function of the applied temperature differential ( $\Delta T$ ), are shown in Figure 2c. The displayed thermoelectric voltages represent the mean of the measured voltage in ten independent measurements, where the error bars represent the standard deviation. The magnitude of the measured thermoelectric voltage increases linearly as the applied temperature differential is increased from 0 K to 12 K in steps of 3 K. Additional calculations indeed confirm that the measured thermoelectric voltage should increase linearly for the range of applied temperature differentials and are described in the SI. The

measured thermoelectric voltage is related to the thermopower of the junction ( $S$ ) by the following expression (see the SI for details):

$$S = S_{Au} - \frac{\Delta V}{\Delta T} \quad (3)$$

Here,  $S_{Au}$  is the thermopower of gold, and  $\Delta V$  is the measured voltage differential between the tip and the grounded substrate. Using this expression and the measured thermoelectric voltages (Figure 2c), the Seebeck coefficient corresponding to junctions based on SS1, SS2, SS3 molecules is found to be  $(+9.8 \pm 0.6) \mu\text{V/K}$ ,  $(+11.7 \pm 1.3) \mu\text{V/K}$ , and  $(+15.4 \pm 1.0) \mu\text{V/K}$  respectively (Table 1). The variation in the measured Seebeck coefficients across experiments arises due to changes in the microscopic details of the metal-molecule contacts.<sup>23</sup> Further, there is a 5% uncertainty in the applied temperature differential<sup>16</sup>, which is also accounted for in the reported standard deviation of the Seebeck coefficients. Control experiments were performed to ensure that the measured thermopower does not arise from Au-Au point contacts. Further details regarding the control experiments are described in the Supporting Information and a previous work<sup>16</sup>.

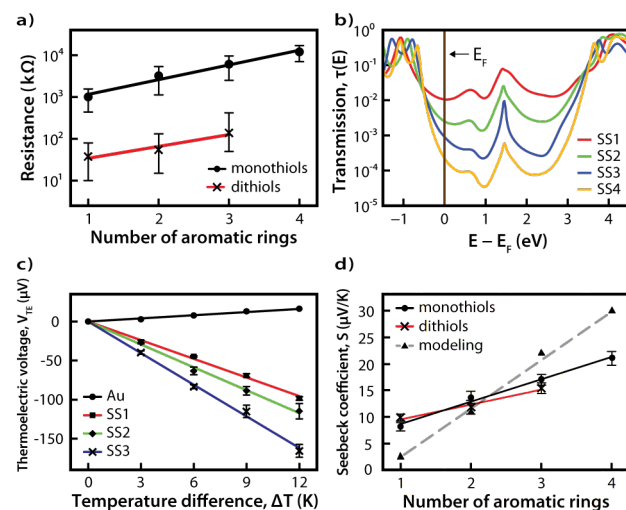


**Figure 2.** a) The measured electrical resistances of monothiol and dithiol junctions containing  $\sim 100$  molecules. b) The computed transmission functions for the Au-aromatic dithiol-Au junctions. c) The thermoelectric voltages obtained for Au-aromatic dithiol-Au junctions are shown along with those obtained for a Au-Au point contact. d) The Seebeck coefficients of the dithiol and monothiol junctions are plotted along with the computed values for the Seebeck coefficient of the dithiol junctions.

It is insightful to note that when the intermolecular interactions are weak, the molecules in a multiple molecule junction act as independent channels. In this case, the multiple molecule junction would indeed have a Seebeck coefficient that is invariant with the number of molecules in the junction. The measured multiple molecule junction (monolayer) Seebeck coefficients in this study are in very good agreement with previous measurements of corresponding single molecule junctions<sup>10</sup> (Table 1). This correlation indicates that the intermolecular interactions in the studied monolayers are small and do not significantly affect the measured Seebeck coefficient.

In our computational studies, the Seebeck coefficient of the molecular junctions are obtained from the transmission function using Equation 2. The slope of the transmission function at  $E_F$  is negative for all the thiol terminated junctions. The resulting positive Seebeck coefficients and the corresponding measured values are plotted in Figure 2d. The increase of the Seebeck coefficient with the number of rings, as indicated by the measurements, is well reproduced by our computational results and is also consistent with recent computational studies<sup>24,25</sup>. Some of the deviations between experiment and modeling may be due to the microscopic variations in the contact details, which are

not addressed by the computational model. Further, molecular vibrations that cause the benzene rings in the molecules to deviate from their equilibrium alignments, which are not considered in this study, also affect transport properties.

No. of rings	Experimentally measured values ( $\mu\text{V}/\text{K}$ )			Computed dithiol values ( $\mu\text{V}/\text{K}$ )
	Monothiols	Dithiols	Previous single molecule dithiol studies <sup>10</sup>	
1	$8.1 \pm 0.8$	$9.8 \pm 0.6$	$8.7 \pm 2.1$	2.4
2	$13.6 \pm 1.2$	$11.7 \pm 1.3$	$12.9 \pm 2.2$	10.8
3	$17.0 \pm 1.0$	$15.4 \pm 1.0$	$14.2 \pm 3.2$	21.9
4	$21.0 \pm 1.3$	–	–	29.9

**Table 1. Experimental and Computational Values of Seebeck Coefficients for Aromatic Thiol based Junctions.** The experimentally measured Seebeck coefficient of the dithiol and monothiol junctions is presented along with the computed Seebeck coefficients of the dithiol junctions. The Seebeck coefficients of single molecule dithiol junctions obtained in an earlier work are also presented for comparison.

*Effect of contact coupling strength on electrical conductance and Seebeck coefficient.* Past theoretical studies<sup>22</sup> have elucidated the effect of contact coupling strength on the thermoelectric properties of junctions. These computational studies suggest that when coupling of a molecular junction with one of the electrodes is weakened, the electrical conductance of the junction decreases significantly whereas the Seebeck coefficient remains relatively invariant. In order to test this hypothesis, we experimentally studied transport properties of junctions fabricated from self-assembled monolayers of monothiol molecules (S1, S2, S3, S4, Figure 1b). The measured electrical resistances of the monothiol molecular junctions are shown in Figure 2a. We estimate that the number of molecules in all junctions is approximately the same, which allows a direct comparison of the junction resistances (see SI for details). These measurements show that the electrical resistance of the monothiol junctions is at least an order of magnitude larger than the corresponding dithiol junctions. A similar trend has been observed in previous studies on aliphatic and aromatic molecular junctions.<sup>13,26</sup> We measured the Seebeck coefficients of the monothiol junctions and list them in Table 1. Remarkably, the change in coupling strength has only a marginal effect on the Seebeck coefficient—the difference in the thermopower of monothiol and dithiol junctions is only a few percent and is in strong contrast with the large difference (an order of magnitude) in the electrical resistance of molecular junctions.

This behavior is well explained using a simple model by Paulsson and Datta<sup>22</sup>. In this picture the transmission function of a weakly bound junction is related to the transmission of a strongly bound junction by a scaling factor ( $0 < c < 1$ ):

$$\tau(E)_{\text{weak}} = c \times \tau(E)_{\text{strong}} \quad (4)$$

In our case, the monothiol and the dithiol junctions represent the weakly and strongly bound junctions, respectively. Considering Equations 2 and 4, it is evident that decreased contact coupling lowers the electrical conductance, whereas the Seebeck coefficient remains invariant to changes in the coupling. Our experimental data provides the first convincing evidence that this simple model<sup>22</sup> can qualitatively capture the effect of weakening the coupling with one of the contacts.

*Effect of contact chemistry on the Seebeck coefficient.* Recent computational<sup>27-29</sup> and experimental work<sup>11,30,31</sup> suggests that end group chemistry provides an attractive route for tuning the electronic energy levels of the junction relative to the chemical potential. Here, we explore the prospect of changing the sign of the Seebeck coefficient by end group chemistry. The positive Seebeck coefficients realized with thiol terminated junctions suggest p-type transport, which is associated with the HOMO being the closest level to the Fermi energy. Indeed, we confirm this by the calculated transmission, which shows that transport is

dominated by the HOMO electronic channel (Figure 2b). A negative sign of the Seebeck coefficient is expected to be realized with the opposite case of LUMO dominated transport. In fact, it has been hypothesized that n-type transport can be realized with isocyanide end groups.<sup>29</sup> In order to test this hypothesis, we designed experiments where monolayers were created from an isocyanide ( $-\text{NC}$ ) terminated aromatic molecule (NC3, Figure 1b).

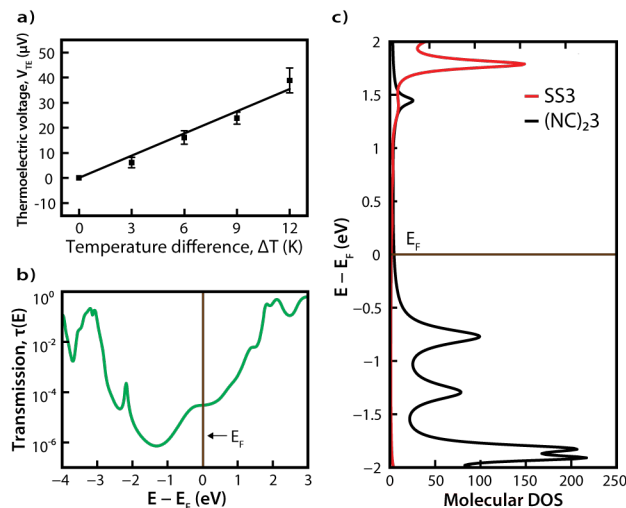


**Figure 3.** a) The measured thermoelectric voltages of Au-NC3-Au junctions. b) The computed transmission functions for the Au-aromatic diisocyanide-Au junction. c) Molecular electronic density of states (DOS) around the chemical potential in the SS3 and (NC)<sub>2,3</sub> junctions.

The thermoelectric voltages measured for isocyanide terminated junctions are shown in Figure 3a. The measured thermoelectric voltages indicate a negative Seebeck coefficient of  $-1.0 \pm 0.4 \mu\text{V}/\text{K}$ . The sign of the Seebeck coefficient confirms that transport in the isocyanides is n-type. This result is particularly insightful because previous electrical transport studies<sup>27</sup> of isocyanide junctions were unable to determine whether the HOMO or the LUMO is closer to  $E_F$ .

We model the transport properties of the three ringed diisocyanide junctions to analyze the sign dependence of the thermopower on the contact (Figure 3b). For modeling simplicity, we continue to relate the Seebeck coefficient of the mono functionalized molecular junction to a model that involves two end groups (NC)<sub>2,3</sub>. This modeling scheme is justified by our observation of the invariance of the Seebeck coefficient on the coupling strength. The computed transmission function shows that transport in diisocyanide junctions is dominated by the LUMO channel, resulting in n-type transport. The Seebeck coefficient calculated for the 3 ring isocyanide junction ( $-1.6 \mu\text{V}/\text{K}$ ) matches in sign with the experiments, and has a magnitude comparable to the experimentally measured value of  $-1.0 \pm 0.4 \mu\text{V}/\text{K}$ .

The negative Seebeck coefficient of the isocyanide junction is in contrast to the positive coefficient of the corresponding thiol terminated junction. We relate the sign reversal to the electronic structure of the junction by observing the electronic density of states (DOS). The electronic DOS in the molecular region for SS3 and (NC)<sub>2,3</sub> junctions are plotted in Figure 3c. The DOS for the SS3 junction shows that transport is dominated by orbitals below the chemical potential (p-type), resulting in a positive thermopower. In contrast, the electronic DOS of (NC)<sub>2,3</sub> junctions shows that transport is dominated by orbitals above the chemical potential (n-type), resulting in a negative thermopower. Further details on the orbitals related to the electron transport channels are provided in the SI.

It is interesting to note that when the contact coupling is reduced by removing one of the thiol groups, the Seebeck coefficient is relatively invariant (Table 1). However, changing the end groups from thiol to

1 isocyanide changes not only the magnitude of the Seebeck coefficient  
2 but also its sign. This result can be qualitatively understood by noting  
3 that when a completely different end group (–NC as opposed to –SH)  
4 couples a molecule to an electrode, the electronic structure of the mo-  
5 lecular junction is radically changed, as demonstrated by our calcula-  
6 tions, resulting in large changes in the Seebeck coefficient. In contrast,  
7 when one of the contacts with the electrodes is weakened, we believe  
8 that the local density of states in the molecular junction remains quali-  
9 tatively similar to that of a junction that is strongly bound to both the  
10 electrodes, resulting in a relatively invariant Seebeck coefficient. Vali-  
11 dating this hypothesis via systematic computational studies is the focus  
12 of our future work. We note that the effect of end groups on the sign of  
13 the thermopower was also observed in a previous experimental study  
14 by one of us in collaboration with others<sup>11</sup> using cyanide (–CN) termi-  
15 nated molecules. In contrast, the current study of isocyanide (–NC)  
16 terminated junctions not only explores the applicability of another end  
17 group to tuning thermoelectric properties but—more importantly—  
18 probes the relationship between electronic structure and the sign of  
19 thermopower.

20 To summarize, we have studied thermoelectric properties of mo-  
21 lecular junctions via a combined experimental and computational ap-  
22 proach. Our studies indicate that the thermopower (Seebeck coeffi-  
23 cient) of thiol terminated junctions are positive in sign and increase  
24 linearly with the length of the molecule. Our computational studies  
25 associate the positive sign of the junction with the proximity of the  
26 HOMO to the chemical potential. We also show that when the cou-  
27 pling of the molecule with one of the electrodes is reduced, the electri-  
28 cal conductance of junctions decreases dramatically, whereas, the  
29 thermopower remains relatively invariant. Further, we show that for an  
30 isocyanide terminated junction the sign of the thermopower is nega-  
31 tive. Our computational studies demonstrate that this change is due to  
32 transport being dominated by the LUMO based channel in the isocya-  
33 nide junction. These results demonstrate the possibility of tuning the  
34 thermoelectric properties of molecular junctions via contact chemistry  
35 and molecular structure

36 ACKNOWLEDGMENT. A.T. was supported by DOE-BES as part  
37 of an EFRC at the University of Michigan (DE-SC0000957). S.S. was  
38 supported by the U.S. Department of Energy, Office of Basic Energy  
39 Sciences, Division of Materials Sciences and Engineering under Award  
40 DE-SC0004871. B.D.D. gratefully acknowledges support by a DOE-  
41 BES award through the Chemical sciences Geosciences and Bio-  
42 sciences Division (DE-SC0004924).

43 SUPPORTING INFORMATION AVAILABLE. Computational  
44 methodology, experimental procedures, control experiments, charac-  
45 terization. This material is available free of charge via the Internet at  
46 <http://pubs.acs.org>.

#### 47 REFERENCES.

- 48 (1) Guisinger, N. P.; Greene, M. E.; Basu, R.; Baluch, A. S.; Hersam, M.  
49 C., *Nano Lett.* **2004**, *4*, 55-59.
- 50 (2) Chabinyk, M. L.; Chen, X. X.; Holmlin, R. E.; Jacobs, H.; Skulason,  
51 H.; Frisbie, C. D.; Mujica, V.; Ratner, M. A.; Rampi, M. A.;  
52 Whitesides, G. M., *J. Am. Chem. Soc.* **2002**, *124*, 11730-11736.

- 53 (3) Xu, B. Q.; Li, X. L.; Xiao, X. Y.; Sakaguchi, H.; Tao, N. J., *Nano Lett.*  
54 **2005**, *5*, 1491-1495.
- 55 (4) Song, H.; Kim, Y.; Jang, Y. H.; Jeong, H.; Reed, M. A.; Lee, T.,  
56 *Nature* **2009**, *462*, 1039-1043.
- 57 (5) Bergfield, J. P.; Solis, M. A.; Stafford, C. A., *ACS Nano* **2010**, *4*,  
58 5314-5320.
- 59 (6) Bergfield, J. P.; Stafford, C. A., *Nano Lett.* **2009**, *9*, 3072-3076.
- 60 (7) Finch, C. M.; Garcia-Suarez, V. M.; Lambert, C. J., *Phys. Rev. B*  
**2009**, *79*, 033405.
- (8) Macia, E., *Phys. Rev. B* **2007**, *75*, 035130.
- (9) Xu, B.; Tao, N., *Science* **2003**, *301*, 1221-1223.
- (10) Reddy, P.; Jang, S. Y.; Segalman, R. A.; Majumdar, A., *Science* **2007**,  
*315*, 1568-1571.
- (11) Baheti, K.; Malen, J. A.; Doak, P.; Reddy, P.; Jang, S. Y.; Tilley, T.  
D.; Majumdar, A.; Segalman, R. A., *Nano Lett.* **2008**, *8*, 715-719.
- (12) Venkataraman, L.; Klare, J.; Nuckolls, C.; Hybertsen, M.;  
Steigerwald, M., *Nature* **2006**, *442*, 904-907.
- (13) Engelkes, V. B.; Beebe, J. M.; Frisbie, C. D., *J. Am. Chem. Soc.* **2004**,  
*126*, 14287-14296.
- (14) Malen, J. A.; Doak, P.; Baheti, K.; Tilley, T. D.; Segalman, R. A.;  
Majumdar, A., *Nano Lett.* **2009**, *9*, 1164-1169.
- (15) Nitzan, A.; Ratner, M. A., *Science* **2003**, *300*, 1384-1389.
- (16) Tan, A.; Sadat, S.; Reddy, P., *App. Phys. Lett.* **2010**, *96*, 013110.
- (17) Beebe, J. M.; Engelkes, V. B.; Miller, L. L.; Frisbie, C. D., *J. Am.*  
*Chem. Soc.* **2002**, *124*, 11268-11269.
- (18) Imry, I.; Landauer, R., *Rev. Mod. Phys.* **1999**, *71*, S306.
- (19) Prociuk, A.; Van Kuiken, B.; Dunietz, B. D., *J. Chem. Phys.* **2006**,  
*125*, 204717.
- (20) Xue, Y.; Datta, S.; Ratner, M. A., **2002**, *Chem. Phys.* *281*, 151.
- (21) Yaliraki, S. N.; Roitberg, A. E.; Gonzalez, C.; Mujica, V.; Ratner, M.  
A., *J. Chem. Phys.* **1999**, *111*, 6997.
- (22) Paulsson, M.; Datta, S., *Phys. Rev. B.* **2003**, *67*, 241403R.
- (23) Malen, J. A.; Doak, P.; Baheti, K.; Tilley, T. D.; Majumdar, A.;  
Segalman, R. A., *Nano Lett.* **2009**, *9*, 3406-3412.
- (24) Ke, S.-H.; Yang, W.; Curtarolo, S.; Baranger, H. U., *Nano Lett.* **2009**,  
*9*, 1011-1014.
- (25) Quek, S. Y.; Choi, H. J.; Louie, S. G.; Neaton, J. B., *ACS Nano*,  
**2011**, *5*, 551-557.
- (26) Hong, S.; Reifengerger, R.; Tian, W.; Datta, S.; Henderson, J. I.;  
Kubiak, C. P., *Superlattices and Microstructures* **2000**, *28*, 289-303.
- (27) Ke, S.-H.; Baranger, U. H.; Yang, W. *J. Am. Chem. Soc.*, *2004*, *126*  
*(48)*, pp 15897-15904
- (28) Mishchenko, A.; Vonlanthen, D.; Meded, V.; Burkle, M.; Li, C.;  
Pobelov, I. V.; Bagrets, A.; Viljas, J. K.; Pauly, F.; Evers, F.; Mayor,  
M.; Wandlowski, T., *Nano Lett.* **2010**, *10*, 156-163.
- (29) Xue, Y. Q.; Ratner, M. A., *Phys. Rev. B* **2004**, *69*, 085403.
- (30) Zotti, L. A.; Kirchner, T.; Cuevas, J. C.; Pauly, F.; Huhn, T.; Scheer,  
E.; Erbe, A., *Small* **2010**, *6*, 1529-1535.
- (31) Mishchenko, A.; Zotti, L. A.; Vonlanthen, D.; Burkle, M.; Pauly, F.;  
Cuevas, J. C.; Mayor, M.; Wandlowski, T., *J. Am. Chem. Soc.* **2010**,  
*133*, 184-187.

Table of Contents Artwork:

